JPE 11-4-11

Development of a Unified Research Platform for Plug-In Hybrid Electrical Vehicle Integration Analysis Utilizing the Power Hardware-in-the-Loop Concept

Chris S. Edrington†, Oleg Vodyakho*, and Brian A. Hacker*

†* Center for Advanced Power Systems, Florida State University, Florida, United States

Abstract

This paper addresses the establishment of a kVA-range plug-in hybrid electrical vehicle (PHEV) integration test platform and associated issues. Advancements in battery and power electronic technology, hybrid vehicles are becoming increasingly dependent on the electrical energy provided by the batteries. Minimal or no support by the internal combustion engine may result in the vehicle being occasionally unable to recharge the batteries during highly dynamic driving that occurs in urban areas. The inability to sustain its own energy source creates a situation where the vehicle must connect to the electrical grid in order to recharge its batteries. The effects of a large penetration of electric vehicles connected into the grid are still relatively unknown. This paper presents a novel methodology that will be utilized to study the effects of PHEV charging at the sub-transmission level. The proposed test platform utilizes the power hardware-in-the-loop (PHIL) concept in conjunction with high-fidelity PHEV energy system simulation models. The battery, in particular, is simulated utilizing a real-time digital simulator (RTDS^{TM}) which generates appropriate control commands to a power electronics-based voltage amplifier that interfaces via a *LC-LC*-type filter to a power grid. In addition, the PHEV impact is evaluated via another power electronic converter controlled through dSPACE^{TM}, a rapid control systems prototyping software.

Key Words: Active front-end unit, Plug-in hybrid electrical vehicle, Power-hardware-in-the-loop, Voltage source inverter

I. Introduction

Plug-in hybrid electric vehicles (PHEVs) utilize battery packs consisting of multiple cells. These batteries have a wide voltage range depending on vehicle type and application [1]–[6]. These multi-celled battery packs can consume substantial amounts of power from the charging station in which they are connected to when the battery state of charge is depleted [3]. A few vehicles connected to the grid via a battery charger may not have a substantial impact; however, at high vehicle penetration levels the impact on the grid could be considerable and thus warrants investigation.

Most utilities have a generation capacity that exceeds the power required during normal operating conditions; however, the replacement of conventional vehicles by PHEVs certainly will result in an unplanned increase in demand. This increased nonlinear power demand could lead to such problems as voltage sag, transmission line temperature increase, harmonics, and instability of the power system. In order to answer these questions, a flexible experimental environment is developed in the laboratory that can be adapted to emulate multiple PHEVs being charged at random time intervals on a single source in order to model how a commercial charging station would supply energy to a group of PHEVs; and subsequently measure this impact on the grid system to which it is connected.

The primary motivation of this work is to develop a test platform which can be utilized to conduct research experiments involving advanced PHEV control system strategies, PHEV integration or a combination of the aforementioned. Using the proposed concept will substantially de-risk the instantiation of PHEV integration experiments, especially for scenarios where the multiple PHEVs are utilized at appreciable power levels. Furthermore, it eliminates the need to obtain the hardware that is modeled within the virtual environment (provided the models are sufficiently validated); thus ultimately lowering cost and risk.

Additionally, this work creates a robust test platform that can be used to analyze and observe the different effects from the implementation of various PHEV charging control strategies.

Manuscript received Jan. 1, 2011; revised May 26, 2011
Recommended for publication by Guest Associate Editor Byoung-Kuk Lee.
† Corresponding Author: edrington@caps.fsu.edu
Tel: +1-850-645-7213, Fax: +1-850-645-7213, Florida State University
* Center for Advanced Power Systems, Florida State University, United States

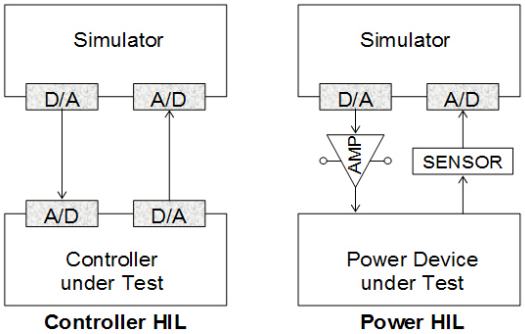

Fig. 1. Structural distinction between CHIL and PHIL simulations.

II. Power Hardware-in-the-Loop Concept and PHEV Battery Modeling

A. Power Hardware-in-the-Loop Concept

Integration of PHEVs, which are connected via power electronic interfaces into the power grid, presents a challenging problem from an impact analysis point of view. While off-line simulation and modeling significantly help in preparing a new product or prototype for field deployment, thorough testing of the hardware under dynamic and transient conditions is essential for the transition of technology from the experimental phase to prototype and, subsequently, product phase. The method of real-time simulation of electric power systems and its application in PHIL experiments is a very powerful tool in this process. In PHIL simulation, a realistic environment for a device is represented on a real-time simulator and interfaced to the device under test through power electronics-based amplifiers. Feedback of the response from the device is then used to complete the control loop, providing a means for the device to fully interact with the simulated environment. PHIL is an extension of the Controller Hardware-in-the-loop (CHIL) simulation method which is widely applied for investigating the real-time behavior of controller and protection equipment. The different structures of CHIL and PHIL simulations are illustrated in Fig. 1 [7].

Since in a CHIL simulation the signals exchanged between the hardware and the simulator are low-power control signals that are usually within the range of +/- 10V, 0 $\sim$ 100mA, commercial digital / analog (D/A) or analog / digital (A/D) converters suffice for the interface.

In contrast, a PHIL simulation of satisfactory accuracy requires a high precision interface amplifier (AMP in Fig. 1). In order to represent the PHEV grid impact from a simulation, a power coupling network is necessary to interface power exchange. In this paper, a PHEV battery and load dynamics are simulated with a real-time digital simulator (RTDS^{TM}), which generates appropriate control commands to a power electronics-based voltage amplifier that interfaces to a power grid via a *LC-LC*-type filter. The voltage amplifier and its passive filter represent a PHEV, establishing a novel unified research platform for PHEV integration analysis.

It should be noted however that imprecision present in the amplified signal, caused by time delays, nonlinearities, sensor noise, and noise injection caused, for example, by power electronic switching within the amplifier, could result in significant simulation error and even instability so detailed system study is required when designing the power coupling network [8].

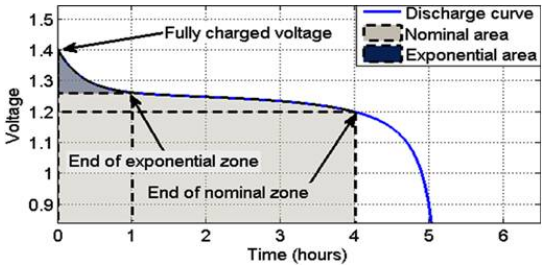

Fig. 2. Nominal current discharge characteristics of a battery.

B. PHEV Battery Modeling

Using an energy storage system comprised of multiple battery cells is a popular proposed way of providing propulsion for PHEVs. Although there is multiple battery cells involved, the energy storage system will act as a single battery and, therefore, can be modeled as such. The ability to model an energy storage system with multiple battery cells as a single battery is an important simplification that has been made in this work, especially since energy systems are complex and usually contain proprietary information that cannot be easily obtained in order to build a model. Through this simplification, the ability to utilize experimental data from an actual energy storage system has been made possible. In order to implement this energy system from a PHIL aspect, it is necessary to develop a real-time battery model in order to accurately reproduce the charging/discharging characteristics of the physical system.

Multiple battery model topologies were considered for the development of the charging system. Battery modeling has been a commonly researched topic with several papers published proposing a variety of models, both mathematical and circuit-based [1]–[5]. In this work, a mathematical model was developed that incorporates the full charge/discharge curve characteristics. The mathematical model is a representation based on Shepherd's equation that was derived in order to explain the nonlinear relationship between the state-of-charge (SOC) and the voltage at the terminals of the energy storage system. This polynomial shaped curve depicting the voltage-time relationship is shown in Fig. 2.

Fig. 2 illustrates the discharge curve of a 5 Ah, 1.2 V nominal voltage battery from an initial completely charged state to a completely discharged final state. As shown in Fig. 2, the voltage curve of a battery during charging/discharging contains three main processes that take place: an exponential drop from full charge as the battery begins to discharge, a linear section about the rated voltage where the battery is typically operated, and a nonlinear section where the battery approaches its completely discharged state. Fig. 3 shows the voltage discharge curves as in Fig. 2, of the experimentally tested energy storage system; however, they are plotted against the amount of charge transferred from the battery as opposed to time. It should be noted, that the curves were plotted against discharge in order to obtain the correlating SOC at specific points along the voltage curve. These points are indicated by the numerically labeled points in Fig. 3.

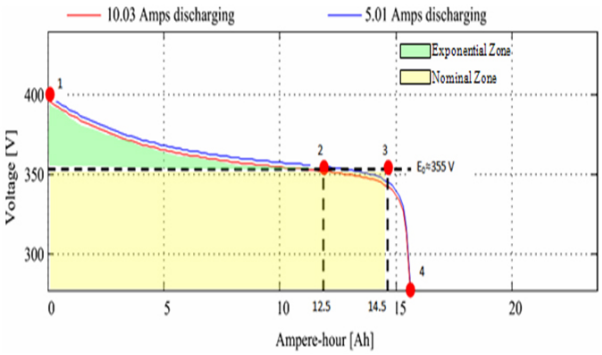

Fig. 3. Voltage discharge curve of energy system with key points.

Each of the indicated points has an importance in expressing the characteristics of the energy storage system model development. Four values must be obtained for the purpose of mathematically modeling the system: voltage at full charge (E_{Full}, point 1), voltage and SOC at the end of the exponential zone (E_{Exp}, point 2), voltage and SOC at the end of the nominal zone (E_{Nom}, point 3), and total battery charge capacity (Q, point 4). Obtaining these values enables the calculation of the coefficients in Shepherd's equation. The coefficients are commonly referred to as A, B, and K and are calculated using the expressions in (1)-(3) where Q represents the charge capacity of the battery.

$$A = E_{Full} - E_{Exp} \tag{1}$$

$$B = \frac{3}{Q_{Exp}} \tag{2}$$

$$K = \frac{(E_{Full} - E_{Exp} + A \cdot (\exp(-B \cdot Q_{Nom}) - 1) \cdot (Q - Q_{Nom}))}{Q_{Nom}} \tag{3}$$

Coefficient A is defined as the exponential zone amplitude, with units of volts, and can be calculated by subtracting the voltage amplitude at the end of the exponential zone from the voltage at full charge as in (1). Coefficient B is defined as the exponential zone time constant inverse, with units of Ah^{-1}, and can be calculated using the charge at the end of the exponential zone as in (2). Coefficient K is defined as the polarization voltage, with units of volts and can be calculated as shown in (3). Shepherd's equation, as given in (4), contains the coefficients that were obtained in order to model the energy storage system. Note that Shepherd's equation consists of three main parts that describe the three main sections of the charge/discharge curve of a battery.

$$E = E_0 - K \cdot \frac{Q}{Q - \int I_{Batt}\, dt} + A \cdot \exp(-B \cdot I_{Batt} t) \tag{4}$$

Essentially, Shepherd's equation states that the voltage at the terminals of the battery, E, is equal to the nominal voltage, E_0, minus the nonlinear zone voltage, plus the exponential zone voltage. The existence of the exponential zone voltage term and nonlinear zone voltage term in Shepherd's equation allows the equation to capture the natural polynomial shape of the voltage curve produced as the battery is charged/discharged. Whether or not the exponential zone voltage term or nonlinear zone voltage term dominates the equation, and dictates the shape of the curve, depends on multiple parameters including the amount of current and how long it has been flowing.

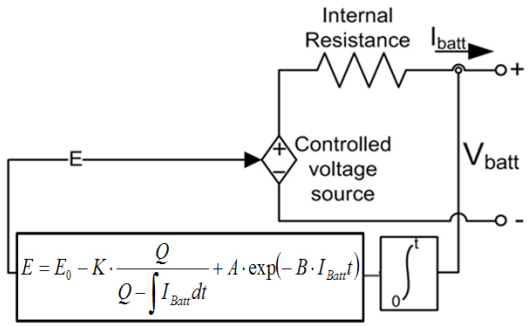

Fig. 4. Energy storage system model representation in simulation environment.

To complete the model information must be obtained regarding the internal resistance of the energy storage system. The internal resistance can be acquired from the manufacturer's specification sheet or experimentally determined through impedance spectroscopy [4]–[6]. Unfortunately, internal resistance of a battery is not a constant value and depends on many factors such as temperature and current magnitude.

The internal resistance for the energy storage system modeled for this research effort was obtained under nominal conditions using impedance spectroscopy since the model being used to simulate the system neglects temperature effects and unordinary dynamic restrictions that more complex models have the ability to address. Modeling these effects would not necessarily be beneficial in this work since the systems will be operated well within their rated values and not subjected to any transient loading conditions.

Substituting the calculated parameters into Shepherd's equation, the mathematical model can be incorporated as a control feedback network to the electrical circuit modeling the energy storage system. The electrical portion of the system model is represented as a simple series circuit with a dependent voltage source and a resistor. The dependent voltage source is used to model the open-circuit voltage while the resistor in series with this source is used to represent the internal resistance of the physical system. The complete model is shown in Fig. 4.

The model is configured such that the current being drawn from/supplied to the energy storage system is measured with a current probe, integrated with respect to time to obtain a continuously compounding rate of charge/discharge, and substituted into Shepherd's equation.

Shepherd's equation is then used to calculate the voltage command, E, that is sent to the dependent voltage source to represent the voltage at the terminals of the energy storage system.

III. Establishment of Experimental Research Platform

The general PHEV power interface configuration shown in Fig. 5 contains the grid connection, charging station, and PHEV. To accomplish the aforementioned setup, two three-phase power converters were utilized; one converter utilizes the (RTDS^{TM}) simulation environment for the PHIL experiment and second converter utilizes the dSPACE^{TM} simulation

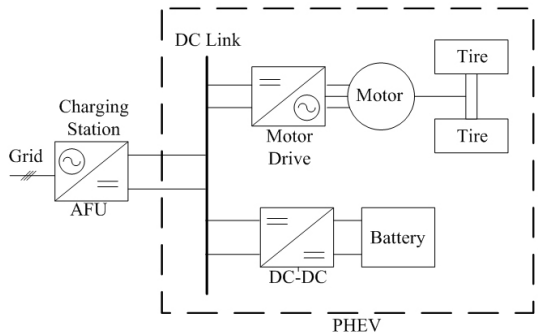

Fig. 5. General PHEV interface configuration.

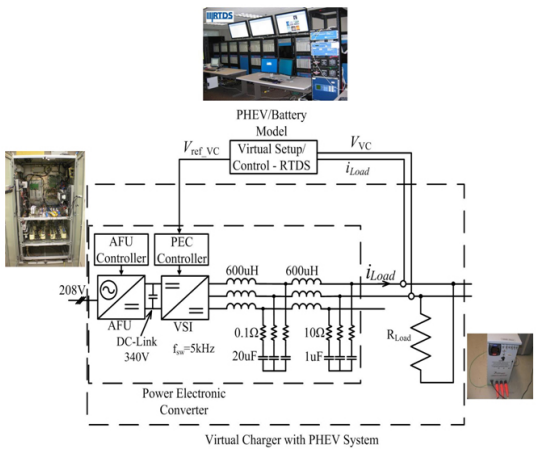

Fig. 6. Proposed research platform with RTDS^{TM}.

environment, a rapid control systems prototyping software [9]-[10]. The converter that utilizes RTDS^{TM} is used first to observe the effects of charging PHEVs on the grid using the battery model that was developed. The converter controlled with dSPACE^{TM} is utilized for detailed harmonic analysis of PHEV load current and its impact on a power grid.

A. RTDS^{TM} Implementation

First, the 208 V-three-phase converter (25 kVA) representing a virtual charger (VC) is utilized for PHEV impact studies a shown in Fig. 6. The converter consists of an active front unit (AFU), which is interconnected with the voltage source inverter (VSI) through a common dc-bus (340 V) as shown in Fig. 6. The AFU control circuit consists of six fully controlled IGBT switches (two-level inverter topology), three line inductors on the ac side (not shown in Fig. 6), and a capacitor on the dc side. The conventional sine-triangle PWM is used as a modulation strategy for the AFU. The VSI is based on the same two-level inverter topology as the AFU, controlled with a power electronics controller (PEC) and utilizes a Reference-Carrier-Modulator (RCM), which uses a Reference-Carrier method for calculation of three-phase patterns [11], [12]. The PEC is programmed by an Ethernet connected host PC by means of MATLAB/Simulink^{TM} and the real-time workshop. The switching frequency of the VSI is set to 5 kHz.

In order to achieve the desired VC operation for PHEV impact studies, the previously described battery model based on (4) and an additional control algorithm that form the PHIL experiment are implemented in RTDS^{TM} as shown in Fig. 7.

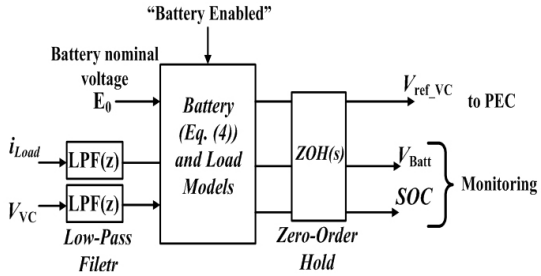

Fig. 7. PHIL control setup implemented in RTDS.

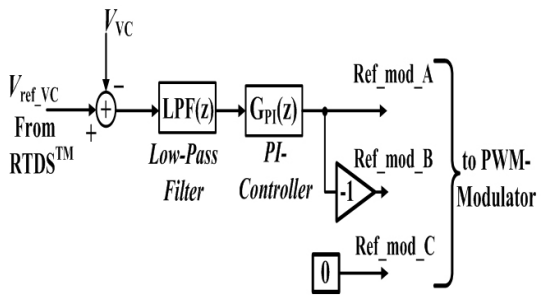

Fig. 8. PEC control algorithm.

Prior to sending the PHEV model references to the PEC, by means of enabling the battery model (signal "Battery Enable"), the battery nominal voltage E_0 needs to be defined first.

The measured VC output voltage (V_{VC}) and load current (i_{Load}) are filtered with a first order low-pass filter (LPF) with a cut-off frequency ω_c and the following transfer function LPF(z):

$$LPF(z) = \frac{P \cdot z + P}{z - D} \tag{5}$$

where the coefficients for the low-pass filter P and D are defined as follows:

$$P = \frac{T_s \cdot \omega_c}{2 + T_s \cdot \omega_c}; \quad D = \frac{2 - T_s \cdot \omega_c}{2 + T_s \cdot \omega_c} \tag{6}$$

and $T_s = 50\mu$s is the sampling period and $\omega_c = 2 \cdot \pi \cdot 10$ Hz.

The RTDS^{TM} is used to regulate the VC output voltage V_{ref_VC} at the experimental bus by providing instantaneous voltage references to the PEC controller of the VSI. This is no longer a discrete time process, so a Zero-Order Hold (ZOH) is introduced in the PHIL control loop as shown in Fig. 7. In addition to the closed-loop mode utilizing the measured load current i_{Load}, the proposed PHIL control setup can operate in open-loop mode by accepting reference current charge/discharge values which can be determined by a user.

The PEC control algorithm is shown in Fig. 8. The PEC is implemented in high speed control tasks required in power converter applications and low speed tasks (converter interaction with plant) in one single processor with a sampling period $T_s = 10\ \mu$s.

The PI controller provides the VC voltage closed-loop control by utilizing a discrete-time domain PI controller. The PI controller is tuned to be very slow in order to avoid the system disturbances. The LPF(z) transfer function is equivalent of (5)-(6).

As shown in Fig. 5, a PHEV structure incorporates a DC-DC converter responsible for scaling the voltage from the charging station to an appropriate level so that the energy storage system

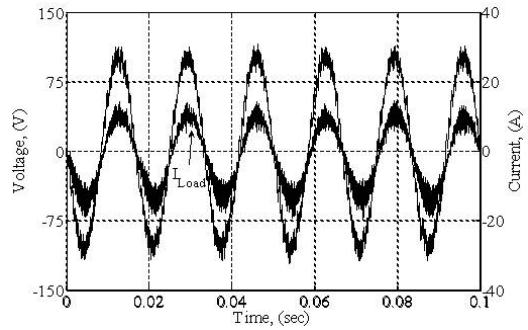

Fig. 9. VSI operation with sinusoidal references.

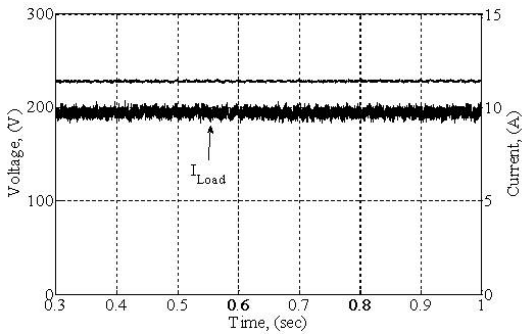

Fig. 10. VSI operation with DC references.

is appropriately managed during charging. Utilizing the VSI, it's possible to reproduce the behavior of a DC-DC converter in a PHEV in order to assist in the development of the VC station.

To accurately represent the DC-DC converter, the VSI switching modulation was modified to produce a DC output so that both the input and output of the VSI were DC quantities. In this case, as shown in Fig. 8, the phase A modulation reference *Ref_mod_A*, and the phase B modulation reference *Ref_mod_B* were set equal in magnitude but opposite in polarity so that they would imitate the positive and negative terminals of a DC system. The aforementioned reference modulation signals are then passed to PWM modulator of a PEC.

Depicted in Fig. 9 is the grid current and load current waveforms of the conventional VSI operation with sinusoidal references. Under this operation the output of the VSI is controlled to generate a sinusoidal output voltage in phase with the grid current, which represents a desired active power flow.

Fig. 10 shows the output voltage and load current waveforms of the proposed VC interface utilizing the DC references used in the PWM modulation of the VSI. Unlike the case with sinusoidal references, the DC references produce a DC load current that is more representative of the DC quantities that would be used to charge the energy storage system of a PHEV.

Once the operation of the VSI had been modified to produce a DC output, the virtual grid interface system can be constructed such that the structure of the VC station and PHEV can be appropriately emulated. The next section discusses the complete configuration of the power hardware and the inclusion of the energy storage system that was modeled in RTDS^{TM}.

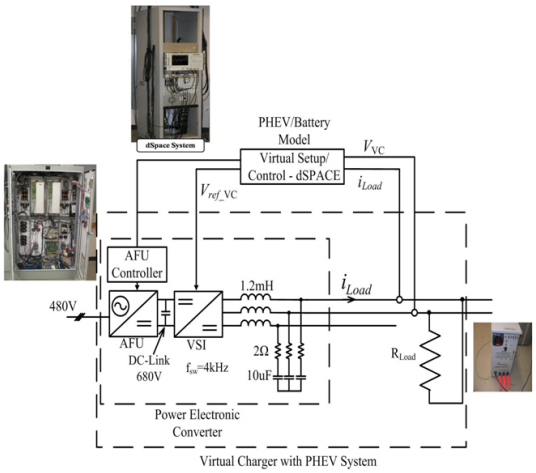

Fig. 11. Proposed research platform with dSPACETM.

The goal of the test platform is to demonstrate the operational characteristics of a charging station and how it would affect the grid. This is accomplished by monitoring the charging curves of each of the PHEV battery models in software and observing the grid current that will be measured at the input side of the VSI, particularly recording the transient qualities of the current waveform during load changes. The active load bank will be changed in decreasing sequential steps such that current between the VSI and load bank is increased so as to represent PHEVs being added to the virtual charger.

B. dSPACE^{TM} Implementation

Similar to the previous converter setup, the dSPACE^{TM}-controlled converter connected to a 480 V-three-phase power grid is used for additional studies of PHEV grid impact as shown in Fig. 11. The dSPACE^{TM} system has direct control over the switching devices of the converter. In contrast to PEC-controlled converter described in the previous section, in this converter setup, the AFU utilizes the hysteresis modulation technique and the VSI adopts a conventional sine-triangle PWM with 4 kHz switching frequency. With the additional ability to control the switching algorithm, this test platform can be configured with a conventional diode rectifier representing a charging station or utilizing an AFU. The results obtained with a diode rectifier and AFU will be evaluated in the next section.

IV. Simulation and Experimental Results

This section presents the selected experimental results of the research platform for PHEV integration studies described above utilizing RTDS^{TM} and dSPACE^{TM} simulation environments. The first section will highlight the results obtained using the RTDS^{TM} simulation environment forming the PHIL experiment and the second section with discuss the results acquired using the dSPACE^{TM}-controlled 480 V-three-phase power converter.

A. RTDS^{TM} Implementation Results

To validate the presented battery model, the VSI was connected directly to a resistive load to perform a controlled

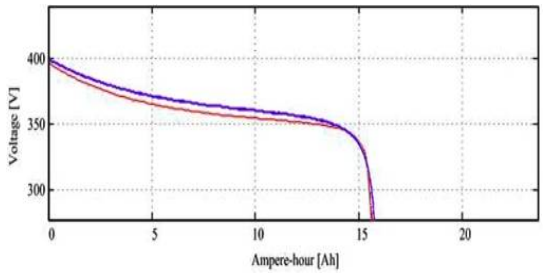

Fig. 12. Validation of software model with model.

discharge test. The test results were then compared to those of the physical energy storage system shown in Fig. 3. To obtain a constant current discharge a simple DC-DC converter was developed in software to control the energy system's current so that it was held constant despite the system's changing voltage throughout its discharge cycle. This control method is an important implementation for the model validation procedure because it allows the system to discharge in a practical manner such that it remains within its rated values. Additionally, this control method prevents fluctuation in current so that the calculated internal resistance of the system is consistent with the actual internal resistance. A comparison between the model developed for real-time simulation and the actual energy storage system is seen in Fig. 12.

In Fig. 12 the two curves are annotated and represent the experimental curve obtained from the energy storage system and the results obtained from the controlled current discharge in simulation, both for the 10.03 A case, respectively. Notice that the simulated curve accurately follows the experimental curve for the majority of the discharge cycle confirming that our model has sufficient fidelity for this case where temperature, dynamics, and extreme charging rates are not considered.

Once validated, the energy system model was used in simulation in conjunction with the experimental test setup in order to analyze the effects on the grid resulting from PHEVs connected to the VC. As shown in Fig. 13, a simple step load test was conducted with sensors measuring the load current, the grid current, and the VC voltage. In the test case, the load was stepped from 15 A to 20 A at approximately 15 s representing an addition of PHEVs to the charger until approximately 65 s at which point the load was stepped down to 15 A representing the removal of those additional vehicles.

It should be noted that the VC voltage in the top plot remains constant regardless of the changes in the load and line current as expected under properly operating control of a VSI. The ability of the AFU to keep the voltage of the VC stable is analogous to a PHEV's charger ability to maintain a constant voltage regardless of the PHEV load it is subjected to within its rated values.

Fig. 14 is a detailed view of the dynamics that the charging station undergoes when a PHEV load is added to the system. Again the top plot displaying the VC voltage undergoes negligible change when introduced to a worst case scenario, a step change in the load. The middle plot shows the 5 A step load increase along with its effects on the power grid current shown in the bottom plot.

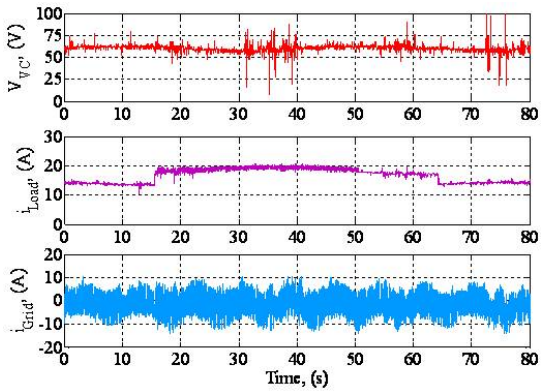

Fig. 13. Representation of PHEVs connecting/disconnecting through load bank step changes. VC voltage (top), load current (middle), grid current (bottom).

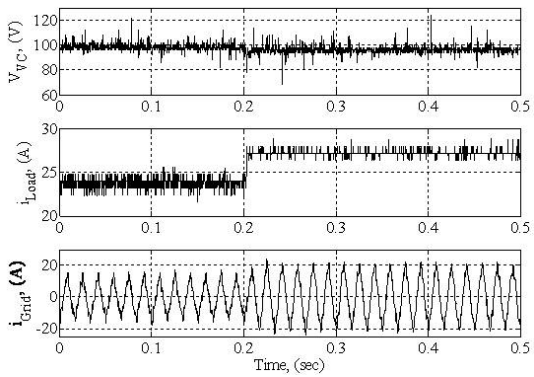

Fig. 14. Transient effects of line current as a result of step load changes; VC voltage (top); load current (middle); grid current (bottom).

Note that the 5 A load increase is representative of at most only one charging PHEV according to the charging infrastructure terms proposed in [13]. However, even at this minimal amount of PHEV introduction the effects are evident on the charger notated by the arrow in bottom plot labeling the initial peak in the line current created by the step change.

Although the initial peak is only approximately 2 A larger than the succeeding peaks, this value could become increasingly large with additional PHEV loads creating an undesirable impact on both the charger, and under extreme conditions, the grid.

Fig. 15 displays the results from the test case where three PHEV models were developed in simulation and charged with different initial connection times. In order to emulate this scenario, the VSI output voltage was set to a DC value and the load was changed in steps. Also, it is evident from Fig. 15 that at the point when the load is increased the next successive PHEV has been connected by observing the increase in the state of charge and voltage, or the decrease in the current sent to each of the models.

Note that the bottom plot does not display the current to each of the vehicles but instead displays the measured current from the VC to the load that is representative of the total charging current. This total current is equal to the individual vehicle current only in the case where one PHEV model is being charged. Although the bottom plot does not show each current, the step increase that occurs each time the load was changed is representative of how much current that single

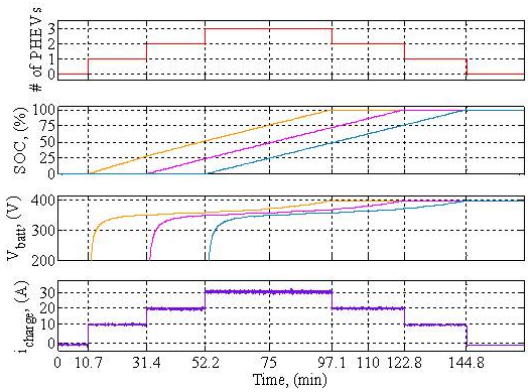

Fig. 15. Charging characteristics for the modeled PHEV energy storage systems.

PHEV is drawing from the system.

As shown in the SOC plot in Fig. 15, the storage system models were charged from 0 to 100% SOC. However, since the energy storage system will never really reach 0 V, each of the modeled energy system's voltages started from a nonzero value as shown in the V_{batt}.

B. dSPACE™ Implementation

In order to estimate the grid impact of PHEV charging utilizing the proposed platform and show the different methods of DC rectification, the setup with a dSPACE™-controlled 480 V-three-phase power converter is used. With the VSI configured for DC mode operation (Fig.16(a)), the load bank was connected to the output of the VSI. As shown in Fig. 16(b), the unmitigated harmonics of a conventional diode rectifier can create negative effects on the grid that range from increased losses to increased conductor temperature, all of which can lead to equipment degradation and consumer expense.

In order to compare the extent of the negative effects contributed by the converter setups, the grid current waveforms for the diode rectifier and AFU cases were obtained for a VSI output of 300 V. Utilizing the same concept for a battery modeling in dSPACE™, the VSI operates in DC mode, creating approximately a 20 A load current. Note that the grid current from the dSPACE™-controlled AFU is more distorted compared to that of the grid current waveform obtained from the PEC-controlled converter. Where the PEC-controlled converter's AFU utilizes a conventional sine-triangle PWM, the dSPACE™-controlled converter's AFU uses a hysteresis current control modulation scheme. This scheme contributes additional distortion due to the 10 A hysteresis band set in the controls which appears on the grid current waveform.

By using a Fourier analysis, the grid current waveform for the diode rectifier and AFU cases were transformed into the frequency domain so that a spectral harmonic analysis could be used to determine their fundamental waveform and the existence of harmonics. The harmonic analysis is limited to the 2500 Hz frequency range since most frequencies that will affect power system components are contained within this range. As shown in Fig. 17, for the diode rectifier case representing a charging station, multiple odd harmonics up to the 29thharmonic at approximately 1740 Hz, excluding the triplen

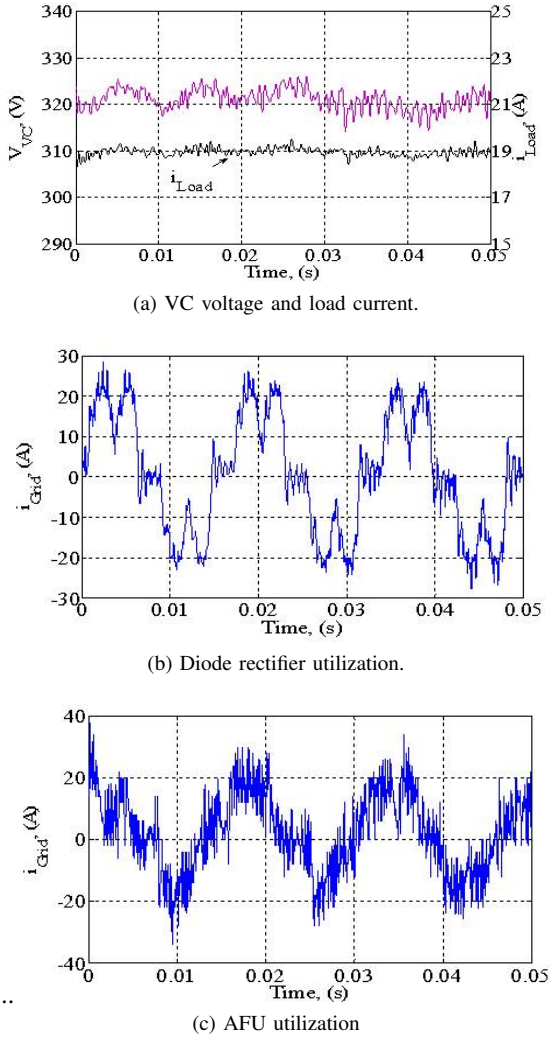

(a) VC voltage and load current.

(b) Diode rectifier utilization.

(c) AFU utilization

Fig. 16. Grid current waveforms during DC mode operation for diode rectifier and AFU case.

harmonics (3rd, 6th, 9th, 12th, etc.) are present in the harmonic spectra. The resulting total harmonic distortion (THD) for the diode rectifier case is approximately 42%, meaning that the total magnitude when the harmonics are summed up is equal to 42% of the magnitude of the fundamental waveform.

The harmonic analysis results for the AFU case show that the odd harmonics that existed in the diode rectifier case are primarily eliminated by the controls except for some small amount of noise due to the switching of the active front end at frequencies below 300 Hz; that which could be reduced by improving the control parameters and the passive filter components of the power converter.

V. Conclusion

This work has presented a novel experimental test setup for the study of V2G interaction by application of the power hardware in the loop methodology. Case examples were provided to illustrate the flexibility of the experimental test bed. It was clearly shown that a real-time digital simulator in conjunction with an appropriate mathematical model of a battery is sufficient to represent the required terminal characteristics and was additionally validated against measured battery data. Furthermore, it was experimentally demonstrated that the battery

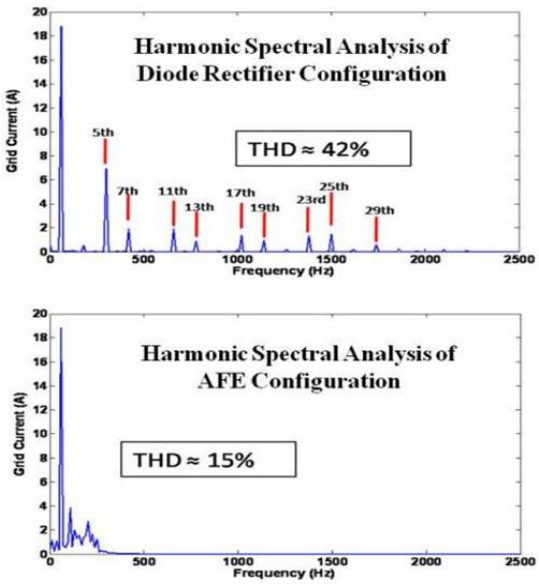

Fig. 17. Harmonic spectral analysis for diode rectifier and AFU case.

model and converter controls of the hardware implementation for the virtual battery charging station correctly emulate the charging scenario of multiple PHEVs. Moreover, the effect that various charging control strategies might have on the grid were utilized as illustrative examples of the potential of the unified research platform for PHEV impact analysis.

REFERENCES

[1] O. Tremblay, L. Dessaint, and A. Dekkiche, "A Generic battery model for the dynamic simulation of hybrid electric vehicles", in *Proc. IEEE Vehicle Power and Propulsion Conference (VPPC-2007)*, pp. 284-289, Sep. 2007.

[2] M. Majima, K. Hanafusa, Y. Oka, G. Tanaka, H. Yoshida, E. Yagasaki, and T. Tada, "Development of 1 kWh (300 Ah) class lithium-ion battery," *J. Power Sources*, Vol. 68, No. 2, pp. 448-450, Oct. 1997.

[3] T. Horiba, K. Hironaka, T. Matsumura, T. Kai, M. Koseki, and Y. Muranaka, "Manganese type lithium ion battery for pure and hybrid electric vehicles," *J. Power Sources*, Vol. 97-98, pp. 719-721, Jul. 2001.

[4] M. Chen and G.A. Rincon-Mora, "Accurate electrical battery model capable of predicting runtime and I-V performance," *IEEE Trans. Energy Convers.*, Vol. 21, No. 2, pp. 504-511, Jun. 2006.

[5] P. Rong and M. Pedram, "An analytical model for predicting the remaining battery capacity of lithium-ion batteries," *IEEE Trans. Very Large Scale Integr. (VLSI) Syst.*, Vol. 14, No. 5, pp. 441-451, May 2006.

[6] P. Mauracher and E. Karden, "Dynamic modeling of lead/acid batteries using impedance spectroscopy for parameter identification," *Journal of Power Sources*, Vol. 67, No. 1-2, pp 69-84, Jul./Aug. 1997.

[7] M. Steurer, C. S. Edrington, M. Sloderbeck, Ren Wei and J. Langston, "A megawatt-scale power hardware-in-the-loop simulation setup for motor drives," *IEEE Trans. Ind. Electron.*, Vol. 57, No. 4, pp. 1254-1260, Apr. 2010.

[8] X. Wu, S. Lentijo, A. Deshmuk, A. Monti, and F. Ponci, "Design and implementation of a power-hardware-in-the-loop interface: a nonlinear load case study," in *Proc. IEEE Applied Power Electronics Conference and Exposition (APEC 2005)*, Vol. 2, pp. 1332-1338, Mar. 2005.

[9] A. Gebregergis and P. Pillay, "Implementation of fuel cell emulation on DSP and dSPACE controllers in the design of power electronic converters," *IEEE Trans. Ind. Appl.*, Vol. 46, No. 1, pp. 285-294, Jan./Feb. 2010.

[10] O. Vodyakho, C. Edrington, M. Steurer, and F. Fleming, "Synchronization of Three-phase converters and virtual microgrid implementation utilizing the power-hardware-in-the-loop concept," in *Proc. IEEE Applied Power Electronics Conference and Exposition (APEC 2010)*, pp.216-222. Feb, 2010.

[11] ABB Automation Technology Products. *ControlIT AC 800PEC Software Guide – Software Version 3.5. ABB*, 2004.

[12] *IP Reference-Carrier-Modulator Rev 3, ABB*, 2004.

[13] Z. Ullah, B. Burford, S. Dillip, "Fast intelligent battery charging: neural-fuzzy approach," *IEEE Aerospace and Electronic Systems Magazine*, Vol. 11, No. 6, pp. 26-34, Jun. 1996.

Chris S. Edrington received his BS in engineering from Arkansas State University in 1999 and his MS and PhD in electrical engineering from the Missouri Science and Technology (formerly University of Missouri-Rolla) in 2001 and 2004, respectively, where he was both a GAANN and IGERT fellow. From 2004∼2007, he was an Assistant Professor of Electrical Engineering in the College of Engineering at Arkansas State University. He currently is an Assistant Professor of Electrical and Computer Engineering with the FAMU-FSU College of Engineering and is the lead for the Energy Conversion and Integration thrust for the Florida State University-Center for Advanced Power Systems. His research interests include modeling, simulation, and control of electromechanical drive systems; applied power electronics; and integration of renewable energy.

Oleg Vodyakho received the degree of Dr.-Ing. from the University (FernUniversität) of Hagen, Germany in 2007, in Electrical Engineering. He joined the Center for Advanced Power Systems, Florida State University in Nov. 2008. He was with the University of Michigan-Dearborn in 2007-2008 as a Post-Doctoral Research Associate. From 2002 to 2003, he was a Fellowship Researcher in the Power Electronics Laboratory at the University of Applied Science Konstanz, Germany. He was with Nokian Capacitors Ltd. as a Research Engineer from 2003 to 2007. His research interests include power electronics system control, power quality issues, application and control of inverters and electric drives.

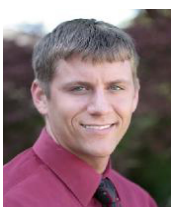

Brian A. Hacker received his BS in engineering from Arkansas State University in 2008 and his MS in electrical engineering from Florida State University in 2010. Currently he is working as a researcher in the Florida State University – Center for Advanced Power Systems. His research interests include modeling, simulation, and integration of renewable energy.